

# Cooling of a Micro-mechanical Resonator by the back-action of Lorentz Force

Ying-Dan Wang, K. Semba, and H. Yamaguchi  
*NTT Basic Research Laboratories, NTT Corporation, 3-1,  
 Morinosato Wakamiya, Atsugi-shi, Kanagawa 243-0198, Japan*  
 (Dated: November 24, 2019)

With a semi-classical approach, we describe an on-chip cooling protocol for a micro-mechanical resonator by a superconducting flux qubit. A Lorentz force, generated by passive back-action of the resonator's displacement, can cool down the thermal motion of the mechanical resonator by applying proper microwave drive on the qubit. We show that this on-chip cooling protocol, with well-controlled cooling power and tunable response time of passive back-action, can be highly efficient. For feasible experimental parameters, the effective mode temperature of a resonator could be cooled from 300 mK down to 1.7 mK.

## I. INTRODUCTION

The rapid development of nanotechnology enables fabrication of micro or nano-mechanical resonator with high frequency, low dissipation and small mass. In the way to observe quantized mechanical motion, thermal fluctuation becomes one of the principal obstacles. The limited cooling efficiency and poor heat conduction at millikelvin temperature of present cryogenic refrigerator has stimulated a number of works to study the active cooling of micromechanical resonator (MR) in classical regime as well as in quantum regime<sup>1,2,3,4,5,6,7,8,9,10,11,12,13</sup>. Among these proposals, the most developed one in experiment is the optomechanical cooling, which has been successfully used to demonstrate cooling<sup>2,3</sup> from room temperature down to 135 mK and from 2.2 K down to 2.9 mK.

In thermal environment, a MR randomly vibrates around its equilibrium position under thermal fluctuation. An effective temperature of a certain mode of MR can be defined by the mean kinetic energy of this mode. The cooling of MR is equivalent to suppress the mean amplitude of Brownian motion, which is the major limitation for precise displacement measurement. The optomechanical cooling of MR is achieved by passive back-action or active feedback of optical forces such as bolometric force<sup>4</sup> and radiation pressure<sup>1,2,3,5,6,7</sup> from laser driven optical cavity.

Instead of introducing optical component, in this paper, we present a cooling protocol for MR in an on-chip superconducting circuit containing three Josephson junctions (JJ). The three-junction superconducting loop forms a flux qubit with much larger energy scale than that of the MR<sup>14,15,16</sup>. The persistent current in this loop exerts a Lorentz force on MR under an in-plane magnetic field<sup>17,18</sup>. This circulating superconducting current is modulated by the thermal motion of the MR through the nonlinear Josephson inductance in a delayed way. Thus the Lorentz force on the MR depends on the motion of the MR itself. This force acts as a passive back-action on the MR just as the radiation pressure in the strategy of optomechanical cooling. The thermal motion of the MR is damped by this back-action force with appropriate parameters. A microwave bias driving the superconducting circuit helps to take away the thermal energy of the resonator. In other words, in the linear response regime, the microwave drive together with the flux qubit in a dissipative environment can be treated as an effective bath with temperature lower than the environmental temperature  $T_0$ . Thereby the mode temperature of the resonator, which is proportional to the mean kinetic energy of the fundamental oscillation mode, is decreased<sup>11,19,20</sup>. The strong and tunable coupling between superconducting current and the displacement of MR is favorable in obtaining highly-efficient and well-controlled cooling. Based on feasible experimental parameters, we also provide detailed analysis on the cooling efficiency of this scheme. The estimation shows that it could be a promising alternative of optomechanical cooling.

This paper is organized as follows: In Sec. II, we describe the setup to implement our cooling scheme. The intuitive picture of this back-action cooling by Lorentz force, together with a general formalism to deal with self back-action cooling is presented in Sec. III. Cooling efficiency of this physical system is found out based on a detailed calculation of the "spring constant" and response time for the Lorentz force in Sec. IV while the lengthy calculation part concerning to the master equation and its steady-state solution are given in Appendix. In Sec. V, according to feasible experimental parameters, cooling efficiency is estimated. Finally in Sec. VI, we discuss the possible advantages, fluctuation and measurement protocol of this cooling protocol.

## II. THE SETUP

The schematics of the setup for this cooling protocol is shown in Fig.1. In the  $x$ - $y$  plane, a doubly-clamped micro-mechanical beam with effective length  $L_0$  is incorporated in a superconducting loop with three small-capacitance Josephson junctions. This mechanical beam can be created from surface-micromachined silicon or carbon nanotube<sup>21</sup>

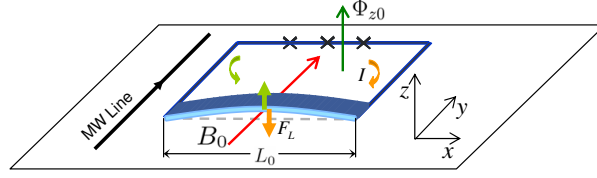


FIG. 1: (Color on line) The schematics of our setup. A doubly-clamped mechanical beam is incorporated in a superconducting loop with superconducting Josephson junction (indicated with crosses) flux qubit. The initial bias in the loop is controlled by magnetic flux  $\Phi_{z0}$  in  $z$  direction. A coupling magnetic field  $B_0$  is imposed on the beam along  $y$  direction and the supercurrent under this magnetic field produces a Lorentz force on the beam. A microwave line introduces microwave bias to the qubit loop. The magnitude of the Lorentz force depends on the motion of the beam through the change of the supercurrent in the loop in a delayed way. This delayed back-action damps the motion of the beam along  $z$  direction and thereby cools down the thermal motion of the beam.

coated with superconducting material, or self-supporting metallic airbridge. The fundamental vibration mode of the beam can be well approximated by a harmonic resonator with oscillation frequency  $\omega_b$ . With a proper bias magnetic flux, two classical stable states of the 3-JJ loop carry persistent current of opposite directions. There is a finite tunneling rate  $\Delta$  between the two persistent-current states due to the Coulomb interaction (throughout this article, we let  $\hbar = 1$ ). For carefully choosing parameters, the subspace spanned by the two states can be well separated from other energy levels and the superconducting loop with Josephson junctions forms a two-level system (superconducting flux qubit)<sup>14,15</sup> and coherent dynamics can be observed<sup>22,23</sup>. Recently, assisted by the third level, microwave-induced cooling of flux qubit has been demonstrated experimentally<sup>24</sup>. The qubit ground state  $|g\rangle$  and excited state  $|e\rangle$  are coherent superpositions of two persistent current states. The energy spacing between the two eigenstates is  $\Omega = \sqrt{\Delta^2 + \varepsilon^2}$  where  $\varepsilon = 2I_p(\Phi_t - \Phi_0/2)$  is the energy spacing of the two classical current states, with  $\Phi_t$  the total magnetic flux in the loop,  $I_p$  the largest persistent current in the loop and  $\Phi_0$  the flux quantum. A microwave bias line is placed close to the circuit and generates microwave drive with frequency  $\omega_d$  on the flux qubit. Under the coupling magnetic field  $B_0$  along  $y$  direction, the persistent superconducting current generates a Lorentz force  $F_L$  on the MR along  $z$  direction. This force couples the flux qubit with the oscillation motion of the MR. In the quantum regime of the MR, this configuration forms a solid-state cavity QED in strong coupling limit<sup>17</sup>.

In the present paper, we concentrate on a different regime where the frequency of MR is much smaller than that of the flux qubit so that the MR can be treated as a classical harmonic oscillator. Since the energy scales of the qubit and the MR are largely different, the dynamics of the composite system can be treated following the line of Born-Oppenheimer approximation: The master equation of the qubit is established by assuming a certain displacement  $z$  of the MR; the steady-state solution for the qubit dynamics is inserted into the classical Langevin equation of the MR to derive the noise spectrum of mechanical displacement.

### III. THE COOLING MECHANISM

In this section, we first present an intuitive understanding for the cooling protocol by the Lorentz force back-action. Based on the classical Langevin equation of the MR, we then proceed to analyze how this back-action leads to the suppression of the random motion of the MR. The explicit form of the Lorentz force back-action in the Langevin equation will be derived in the next section.

The composite system of flux qubit and MR is kept at an environmental temperature  $T_0$  in a dilution refrigerator. The initial constant bias flux of the loop is  $\Phi_{z0}$  along the  $z$  direction. When the MR is displaced by thermal noise to  $z(t)$ , the total magnetic flux in the superconducting loop is changed to  $\Phi_{z0} + B_0 L_0 z(t)$ . In principle, for a MR with aspect ratio close to 1, thermal fluctuation also induces oscillation along  $y$  direction. However, since the magnetic field along  $z$  direction is much smaller than that in  $y$  direction, we only study the motion along  $z$  direction throughout this paper. The increase or decrease of magnetic flux leads to the change of the persistent current  $I$  in the loop after the system reaches a meta-stable state after a response time delay  $\tau_{\text{resp}}$ . Due to the nonlinearity of Josephson junction inductance, the supercurrent at the meta-stable state depends on the total bias magnetic flux and hence depends on the displacement of the MR. Since the Lorentz force is proportional to the supercurrent, the Lorentz force on the MR  $F_L(t + \tau_{\text{resp}})$  depends on the displacement of the MR  $z(t)$  before the time delay. This means that there exists a passive back-action mechanism for the MR: the motion the MR leads to a delayed force on MR itself. We found that, with proper microwave drive, this passive back-action damps the thermal motion of the MR without introducing much additional fluctuation. This cooling protocol is an analog of the self cooling experiments based on optomechanical

coupling<sup>4,25</sup>.

The above intuitive picture can be clearly understood through the study on the dynamics of the MR. To do this, we start from establishing the equation of motion for the MR.

The coupling term in the Hamiltonian of qubit-resonator composite system is<sup>17</sup>

$$H_{\text{int}} = -B_0 L_0 \hat{I} z. \quad (1)$$

where  $\hat{I}$  is the current operator. Then the Lorentz force on the resonator reads

$$\hat{F}_L = -\frac{\partial H_{\text{int}}}{\partial z} = B_0 L_0 \hat{I} \quad (2)$$

Suppose the MR is displaced at  $z$ , after a time delay  $\tau_{\text{resp}}$ , the resulting Lorentz force at meta-stable state  $F_L^{(s)}(z) \equiv \text{Tr}(\rho_q^{(s)}(z) \hat{F}_L)$  depends on  $z$ , where  $\rho_q^{(s)}$  is the reduced density matrix of qubit at meta-stable state. For a small displacement  $z$ , the Lorentz force can be expanded to the linear order of  $z$  as  $F_L^{(s)}(z) = F_0 + k_L z$  with  $k_L$  the effective "spring constant" of the Lorentz force. Since this force is a response to the motion of MR but delayed, its effect on the MR can be described by a delayed response function  $h(t - t') \equiv 1 - e^{-\gamma(t-t')}$  with  $\gamma = 1/\tau_{\text{resp}}$ . Under the Lorentz force, the equation of motion for the MR mode with mass  $m$ , rigidity  $k = m\omega_b^2$  and the inherent damping rate  $\Gamma$  reads<sup>4</sup>

$$m \frac{d^2 z}{dt^2} + m\Gamma \frac{dz}{dt} + kz = F_{th} + \int_0^t \frac{dF_L^{(s)}[z(t')]}{dt'} h(t - t') dt', \quad (3)$$

where  $F_{th}$  is the Brownian fluctuation force which is related to the environment temperature  $\langle F_{th}(t) F_{th}(t') \rangle = 2k_B T_0 m \Gamma \delta(t - t')$ . The stable solution of the motion equation (3) is related to the effective mode temperature  $T_{\text{eff}}$  of the MR by equipartition theorem  $k \langle z^2 \rangle = k_B T_{\text{eff}}$  with  $k_B$  the Boltzman constant. Then the cooling efficiency  $\eta = T_0/T_{\text{eff}}$  can be written as

$$\eta^{-1} = \frac{\Gamma \omega_b^2}{\pi} \int_{-\infty}^{+\infty} \frac{d\omega}{(\omega_{\text{eff}}^2 - \omega^2)^2 + \Gamma_{\text{eff}}^2 \omega^2}, \quad (4)$$

where

$$\begin{aligned} \Gamma_{\text{eff}} &= \Gamma + \Gamma_1, \\ \omega_{\text{eff}}^2 &= \omega_b^2 \left( 1 - \frac{\gamma^2}{\omega^2 + \gamma^2} \frac{k_L}{k} \right). \end{aligned} \quad (5)$$

and

$$\Gamma_1 = \Gamma Q_M \frac{\omega_b \gamma}{\omega_b^2 + \gamma^2} \frac{k_L}{k}, \quad (6)$$

with  $Q_M = \omega_b/\Gamma$  is the quality factor of the MR. For  $|k_L| \ll k$ , the integral can be explicitly carried out as<sup>4</sup>

$$\eta = 1 + Q_M \frac{k_L}{k} \frac{\omega_b \gamma}{\omega_b^2 + \gamma^2}. \quad (7)$$

Eq.(7) has the same form as the one obtained for optomechanical cooling. It can be seen that the sign of  $k_L$  determines the resonator is cooled or heated, i.e. when  $k_L$  is positive, the Lorentz force leads to damping on the motion of the MR and the final temperature is lower than the original one, and vice versa. For positive  $k_L$ , the cooling efficiency increases linearly with  $k_L$ . However, it should be noticed that both the linear response regime and the definition of a single-mode resonator are valid only for  $k_L/k \ll 1$ .

The cooling efficiency is shown by a contour plot in Fig. 2 as a function of two ratios  $\omega_b/\gamma$  and  $k_L/k$ .  $\omega_b/\gamma$  characterizes the ratio between the time scale of response time and oscillation period while  $k_L/k$  is the scaled cooling strength of the passive Lorentz force. The magnitude of the efficiency is indicated by grey level: The higher efficiency is represented by the lighter color. It is seen that the cooling efficiency increases with  $k_L/k$ . In the solid-state system, the coupling strength is usually stronger than its optical counterpart which enables larger  $k_L$ . For a given  $k_L/k$ , the largest cooling efficiency can be achieved by optimizing  $\omega_b/\gamma$ . Those optimal points for each value of  $k_L/k$  are indicated with red dots in Fig. 2. The optimal  $\omega_b/\gamma$  slightly increases with  $k_L$ . For  $k_L/k \ll 1$ , which is the case

we are interested in, the red dots indicate the optimal cooling is realized for  $\omega_b = \gamma$ . This means the largest cooling efficiency is achieved when the response time of back-action matches the oscillation period of the resonator. As we show later, the response time is on the order of the relaxation time of the flux qubit. The qubit relaxation rate ranges from MHz to several tens of GHz, depending on the operating point  $\varepsilon_0$ <sup>26,27</sup>, this implies the flux qubit loop is suitable for cooling resonator with frequency of a broad range. What's more, since the operating point  $\varepsilon_0$  can be controlled by magnetic flux  $\Phi_{z0}$ , the response time of back-action is tunable *in situ*.

#### IV. THE CALCULATION OF THE LORENTZ FORCE

As we discussed in the above section, without considering additional fluctuation, the damping effect of the Lorentz force leads to cooling or heating according to the sign of the effective spring constant  $k_L$ : Positive  $k_L$  leads to cooling while negative  $k_L$  leads to heating. The cooling efficiency is proportional to the magnitude of  $k_L$ . Before proceeding our discussion of cooling efficiency in realistic experiment, it is necessary to obtain the explicit expression of  $k_L$  from the dynamics of the flux qubit system.

The Lorentz force at a meta-stable state for a given displacement  $z$  is

$$F_L^{(s)}(z) = B_0 I_p L_0 \langle \sigma_z \rangle_s \quad (8)$$

where  $\langle \sigma_z \rangle_s$  is the expectation value of  $\sigma_z$  over the steady-state.  $\langle \sigma_z \rangle_s$  can be computed from the dynamics of the driven flux qubit in a dissipative environment. To do this, we start with the effective Hamiltonian of the qubit at a given displacement  $z$  of the MR

$$H_q = \frac{\varepsilon(z)}{2} \sigma_z + \frac{\Delta}{2} \sigma_x + A \sigma_z \cos \omega_d t. \quad (9)$$

Here  $A$  characterizes the amplitude of the microwave drive,

$$\varepsilon(z) = \varepsilon_0 + gz \quad (10)$$

with  $g = -2B_0 I_p L_0$ ,  $\varepsilon_0 = 2I_p \Phi_{z0}$  denotes the initial bias away from the degeneracy point. If the qubit is biased at the degeneracy point,  $\varepsilon_0 = 0$ .

By defining a new set of Pauli operators

$$\begin{aligned} \sigma'_z &= \sigma_z \cos \theta(z) + \sigma_x \sin \theta(z), \\ \sigma'_x &= -\sigma_z \sin \theta(z) + \sigma_x \cos \theta(z), \end{aligned} \quad (11)$$

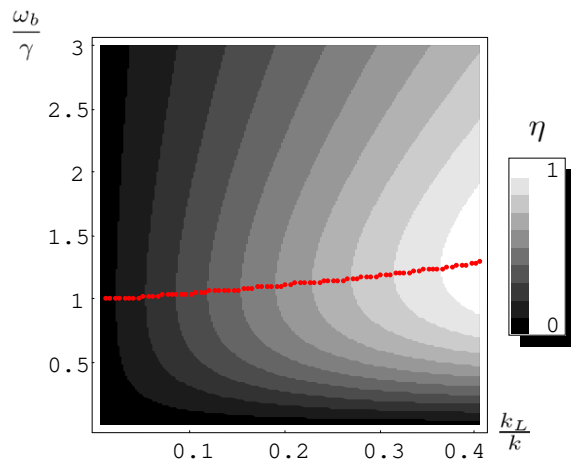


FIG. 2: (Color on line) The dependence of the cooling efficiency on the ratios of  $k_L/k$  and  $\omega_b/\gamma$ . The magnitude of the cooling efficiency is re-scaled and indicated with grey level (higher efficiencies are shown lighter). The other parameters are the same with those used for estimation of cooling efficiency in Sec. V. The red dots indicates the point with largest efficiency at given  $k_L/k$ .

we diagonalize the first two terms of eq.(9) as,

$$H_q = \frac{\Omega(z)}{2} \sigma'_z + A (\sigma'_z \cos \theta(z) - \sigma'_x \sin \theta(z)) \cos \omega_d t, \quad (12)$$

where

$$\cos \theta(z) = \frac{\varepsilon(z)}{\Omega(z)}, \quad \sin \theta(z) = \frac{\Delta}{\Omega(z)}, \quad (13)$$

and

$$\Omega(z) = \sqrt{\Delta^2 + \varepsilon^2(z)} \approx \Omega_0 + \tilde{g}z, \quad (14)$$

with  $\tilde{g} = g\varepsilon_0/\Omega_0$ ,  $\Omega_0 = \sqrt{\Delta^2 + \varepsilon_0^2}$  is the energy spacing between the qubit eigenstates when the displacement  $z$  of the MR is zero. Here we have used the fact that the displacement  $z$  is very small and  $\cos \omega_d t$  is a fast-oscillating term.

If the drive is near-resonant with the qubit frequency  $\Omega_0$ , by making unitary transformation  $U_R = \exp(i\sigma'_z \omega_d t/2)$ , the Hamiltonian (12) in the rotating frame is transformed to be

$$H_R = i \left( \frac{d}{dt} U_R(t) \right) U_R^\dagger(t) + U_R(t) H U_R^\dagger(t) = \frac{\delta(z)}{2} \sigma'_z - \frac{A'(z)}{2} \sigma'_x \quad (15)$$

with  $A'(z) = -A \sin \theta(z)$ ,  $\delta(z) = \delta\omega + \tilde{g}z$  and  $\delta\omega = \Omega_0 - \omega_d$  is the detuning between the qubit free energy and the drive. The term  $A\sigma'_z \cos \theta(z) \cos \omega_d t$  in eq. (12) is neglected because  $\cos \omega_d t$  is a fast-oscillating term since the drive frequency is close to the qubit energy spacing. The diagonalized  $H_R$

$$H_R = \frac{\omega_0(z)}{2} \tilde{\sigma}_z \quad (16)$$

is expressed in another set of Pauli operators

$$\begin{aligned} \tilde{\sigma}_z &= \sigma'_z \cos \beta(z) + \sigma'_x \sin \beta(z), \\ \tilde{\sigma}_x &= -\sigma'_z \sin \beta(z) + \sigma'_x \cos \beta(z), \end{aligned} \quad (17)$$

with

$$\sin \beta(z) = \frac{A'(z)}{\omega_0(z)}, \quad \cos \beta(z) = \frac{\delta(z)}{\omega_0(z)}, \quad (18)$$

and

$$\omega_0(z) = \sqrt{\delta^2(z) + A'^2(z)}. \quad (19)$$

With the above transformation relations, one can derive the master equation for this dissipative flux qubit in rotating frame. Solving the master equation to get its steady-state solution and using the above relations to transform it back to experimental frame, we can obtain  $\langle \sigma_z \rangle_s$  in experimental frame (see Appendix for detail)

$$\langle \sigma_z \rangle_s = -\frac{2 \cos^2 \beta(z)}{1 + \cos^2 \beta(z)} \cos \theta(z) \quad (20)$$

From the last equation of (37), the response time for the supercurrent to reach this value is

$$\tau_{\text{resp}} = \frac{1}{\gamma} = \frac{1}{\Gamma_0} \frac{2}{1 + \cos^2 \beta_0} \quad (21)$$

with  $\cos \beta_0 \equiv \cos \beta(z=0)$ . The response time is on the order of the qubit relaxation time. Shifting qubit bias will change the qubit relaxation time and hence change the response time. On the other hand, similar as the SET-assisted cooling<sup>19</sup>, the response time also depends on the drive detuning and power, this is in contrast to the optomechanical cooling where the response time is always determined by cavity ring-down time.

Since  $z$  is small, the force can be expanded to the linear order of  $z$ :  $F_L^{(s)}(z) = F_0 + k_L z$ , where

$$F_0 = -B_0 I_p L_0 \frac{2 \cos^2 \beta_0}{1 + \cos^2 \beta_0} \cos \theta_0, \quad (22)$$

and the effective spring constant of the Lorentz force is

$$k_L = B_0 I_p L_0 \left( \frac{\partial \langle \sigma_z \rangle_s}{\partial z} \right)_{z=0}. \quad (23)$$

The derivation in the above equation can be explicitly carried out as

$$k_L = \frac{(2B_0 I_p L_0)^2}{\omega_0} \left( \frac{\varepsilon_0^2}{\Omega_0^2} \frac{2\omega_0 \delta\omega A^2}{(\omega_0^2 + \delta\omega^2)^2} + \frac{\omega_0}{\Omega_0} \frac{\Delta^2}{\Omega_0^2} \frac{\delta\omega^2}{\omega_0^2 + \delta\omega^2} \right) \quad (24)$$

where  $\omega_0$  is the value of eq.(19) at  $z = 0$ :

$$\omega_0 = \sqrt{\delta\omega^2 + A^2 \frac{\Delta^2}{\Omega_0^2}}. \quad (25)$$

When the flux qubit is biased near the degeneracy point,  $\varepsilon_0 \sim \Delta$ , in the bracket of eq. (24), the second term is much smaller than the first one due to the small prefactor  $\omega_0/\Omega_0$  (in this case,  $\Omega_0$  is about several gigahertz while the detuning and drive amplitude are about several megahertz) and we neglect the second term

$$k_L \approx (2B_0 I_p L_0)^2 \frac{\varepsilon_0^2}{\Omega_0^2} \frac{2\delta\omega A^2}{(\omega_0^2 + \delta\omega^2)^2}. \quad (26)$$

Eq. (24) represents the explicit form of  $k_L$  expressed by the physical quantities of this system. As we have already noticed, the cooling efficiency is closely related to this effective spring constant  $k_L$ , from this expression, it is ready to study the cooling efficiency of this physical system. Inserting eqs. (24) and (21) into eq. (7), we get the cooling efficiency in this system

$$\eta = 1 + \frac{(2B_0 I_p L_0)^2}{m\omega_b\omega_0} \frac{4Q_M\Gamma_0(1 + \cos^2\beta_0)}{4\omega_b^2 + \Gamma_0^2(1 + \cos^2\beta_0)^2} \left( \frac{\varepsilon_0^2}{\Omega_0^2} \frac{2\omega_0\delta\omega A^2}{(\omega_0^2 + \delta\omega^2)^2} + \frac{\omega_0}{\Omega_0} \frac{\Delta^2}{\Omega_0^2} \frac{\delta\omega^2}{\omega_0^2 + \delta\omega^2} \right). \quad (27)$$

$\eta - 1$ , i.e., the second term of the right part of the above equation, is the change of the cooling efficiency due to the Lorentz force back-action. If  $\eta - 1$  is positive, the back-action leads to cooling, and vice versa. The dependence of  $\eta - 1$  with respect of the drive detuning  $\delta\omega$  and amplitude  $A$  near degeneracy point is shown in Fig. 3. It can be seen that for positive  $\delta\omega$  (red detuning), the cooling regime is reached, and vice versa (however, note that  $\eta < 0$  corresponds to unstable case instead of heating). There is no cooling nor heating for zero drive  $A = 0$ . This is consistent with the optomechanical cooling. However, due to the difference in SU(2) and Heisenberg algebra, for  $\delta\omega > 0$ , the cooling efficiency does not scale with  $A$  monotonically but reaches its maximum at  $A = \sqrt{2}\delta\omega$  as shown in Fig. 4. Physically, this is because too strong drive smashes the back-action mechanism due to its dominant rapid dynamics and even drive the qubit out of the two-level subspace. It is also shown in Fig. 3 that, as  $A$  increases, the variation of the cooling efficiency with respect to  $\delta\omega$  around the peak tends to be much flatter. This feature makes the cooling efficiency robust to operating point fluctuation by increasing the drive amplitude. However, the largest

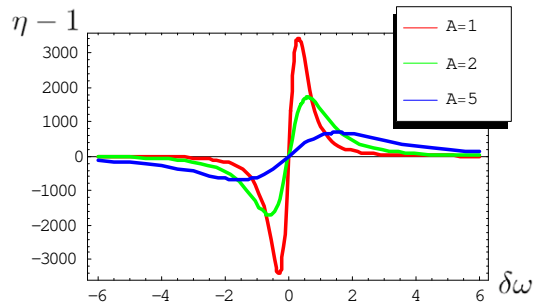


FIG. 3: (Color online) The dependence of the change of cooling efficiency  $\eta - 1$  on the drive frequency  $\delta\omega$  for different drive amplitude.  $\delta\omega$  and  $A$  are in the unit of milliKelvin. All the other parameters are the same as what used in the estimation of cooling efficiency in Sec. V.

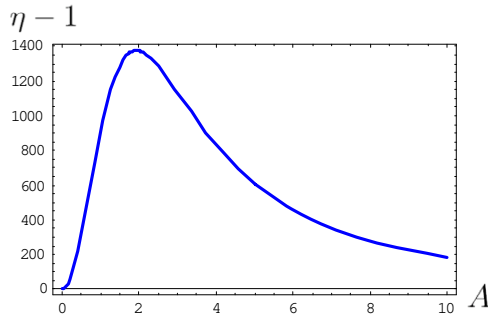


FIG. 4: (Color online) The dependence of the change of the cooling efficiency  $\eta - 1$  on the drive amplitude  $A$  with drive detuning as  $\delta\omega = 1$  mK.  $\delta\omega$  and  $A$  are in the unit of milliKelvin. All the other parameters are the same as what used in the estimation of cooling efficiency in Sec. V.

cooling efficiency also decreases with the increase of  $A$ . Therefore, in experiment, a trade-off is necessary to obtain both stable control and high cooling efficiency.

It is also notable that, if the qubit is biased at the degeneracy point, the second term in eq. (24) can not be omitted. Thus we get a small but finite cooling effect even at the degeneracy point. It is well-known that, based on the first-order perturbation theory, side-band cooling is not possible at qubit degeneracy point. However, driven Rabi oscillation at degeneracy point is demonstrated experimentally<sup>28</sup>. This is explained by fluctuation of operating point or higher-order perturbation theory<sup>29</sup>. It is interesting to observe that this effect is preserved by our semi-classical treatment of back-action cooling. However, based on the treatment of quantized MR, other resonant conditions may be needed to study this phenomenon<sup>29</sup>.

## V. COOLING EFFICIENCY IN PRACTICAL SYSTEMS

After we have obtained the effective spring constant of the Lorentz force and established a relationship of the cooling effect with the back-action mechanism, now it is possible to estimate the cooling efficiency of this protocol for a real system. In order to achieve higher cooling efficiency, it is necessary to increase the mechanical quality factor  $Q_M$  and the coupling strength  $k_L$ . Higher quality factor implies the MR is less affected by the thermal environment. Larger coupling strength means stronger damping by back-action. Besides, as shown in Fig. 2, another crucial factor to improve cooling efficiency is the ratio between the frequency of the MR and the relaxation rate of the flux qubit, i.e., the time scales of the oscillation period and the feedback response from the qubit. Efficient cooling is achieved when the two time scales match each other. In self-cooling experiments with optomechanical coupling, this is one of the main experimental challenges<sup>30</sup>. In our proposal, the response time depends on the relaxation rate of the flux qubit. This rate can be controlled from MHz to GHz by initial bias magnetic flux  $\Phi_{z0}$  along  $z$  direction. By deliberately attaching external impedance to the circuit, the relaxation rate of the flux qubit can be further monitored to match the frequency of the mechanical mode. This feature enables us to optimize the cooling of MR with different mode frequencies and greatly improves the cooling power.

We made our estimation based on a flux qubit loop with Aluminum Josephson junction. In this case, the relaxation time around the degeneracy point of the qubit is on the order of several nanosecond to several microsecond<sup>26</sup>. Hence it is suitable for cooling MR mode with MHz frequency. For example, at environment temperature 300 mK, a flux qubit with  $I_p = 500$  nA,  $\Delta = 5$  GHz,  $\varepsilon_0 = 5$  GHz and the relaxation rate close to the degeneracy point is  $\gamma_0 = 5$  MHz. The qubit is driven by a microwave with  $\omega_d = 7.05$  GHz and  $A = 28.3$  MHz. When the driven qubit is used to cool a doubly-clamped Si beams<sup>31</sup> with  $\omega_b = 6$  MHz,  $k = 0.2$  N/m,  $L_0 = 4.5$   $\mu$ m and quality factor  $Q_M = 10^4$ , Assuming  $B_0 = 4$  mT, we get  $k_L = 7.21 \times 10^{-4}$  N/m. the cooling efficiency  $\eta$  is about  $1.80 \times 10^2$ , which means the effective mode temperature of the MR can be cooled down to about 1.7 mK. Since  $k_L$  is proportional to the square of the coupling magnetic field, increasing  $B_0$  can greatly enhance the cooling power. In principle, the upper limit of  $B_0$  is the critical magnetic field  $B_c$  of the superconducting material in order to preserve superconductivity. For Aluminum,  $B_c \approx 9.9$  mT. But the in-plane magnetic field can be much stronger than this critical value (e.g. even larger than 100 mT<sup>32</sup>) without destroying superconductivity. What's more, suitable arrangement of the magnetic field can make the strong magnetic effect only acts at the MR region while almost canceled at the junction location. This means this cooling protocol is potentially more powerful.

However, one major problem with too strong in-plane magnetic field in experiment is the possible tiny vibration of

the sample with respect to the coupling magnetic field. For strong magnetic field, Significant shift of the operating point may be induced by the tiny vibration. To solve this problem, one may resort to the design of gradiometer-type flux qubit or on-chip magnetic field generating coil<sup>17</sup>.

## VI. DISCUSSIONS

The basic idea of our cooling protocol is an on-chip version for the self-cooling of micro-mirror by optomechanical coupling<sup>30</sup>. The Lorentz force produces a passive back-action on the resonator just as the photothermal force or radiation pressure.

However, the mathematical treatment of a two-level artificial atom is rather different from that of a bosonic field. What's more, practically the two systems have distinct physical nature: (1) The coupling strength in solid-state system is usually stronger than optomechanical system; (2) an on-chip solid-state system without optical component would be favorable in sample fabrication; (3) The coupling between the flux qubit and resonator can be controlled by the applied magnetic field  $B_0$  which is independent of the qubit free Hamiltonian and microwave drive. This is different from the coupling system of the charge qubit and NAMR<sup>33</sup> where the bias voltage  $V_g$  modifies the coupling coefficient as well as the free Hamiltonian of the charge qubit. This feature gives the system more flexibility to increase cooling power and switch on-and-off the cooling process; (4) The frequency of the FP cavity is more than 1 THz to near-resonant with laser. In order to achieve efficient optomechanical cooling for a MHz oscillator, the optical quality factor of the FP cavity should be about  $10^8$ . This calls for mirror with extremely high finesse. But in our case, it is comparatively easier to match the two energy scales since the relaxation rate at the degenerate point is typically on the order of microsecond. (5) The relaxation rate of flux qubit, which determines the response time of back-action, can be modified *in situ* by the bias magnetic flux along  $z$  direction. Although to be biased close to the degeneracy point is advantageous in experiment since the relaxation rate is stable to small fluctuation of flux, in principle for a GHz oscillator, one can work in both  $\gamma \approx \omega_b$  regime and  $\gamma \ll \omega_b$  regime for this Lorentz-force cooling. The latter regime is desirable for cooling towards quantum limit<sup>34</sup>. This implies that our present proposal might be able to cool the MR into its quantum ground state.

In the above discussion, we only considered the damping on the resonator by qubit via the Lorentz force. However, according to the fluctuation-dissipation theorem, fluctuation is always associated with dissipation. Additional fluctuation is also induced by the back-action of the qubit system. For a more comprehensive description, we need to take this fluctuation into account. The additional fluctuation can be represented by an effective temperature  $T_1$ . Therefore, the resonator is effectively in contact with two different baths<sup>11,19,20</sup>, one is the real environment with temperature  $T_0$ , damping rate  $\Gamma$  and the other is the effective bath with effective temperature  $T_1$ , damping rate  $\Gamma_1$ . Physically, the effective bath is formed by the lossy qubit under microwave drive. The temperature of the MR reaches a balance between the two baths as

$$T_{\text{eff}} = \frac{\Gamma T_0 + \Gamma_1 T_1}{\Gamma + \Gamma_1}. \quad (28)$$

The near-resonant microwave drive largely suppresses the fluctuation (see Appendix)

$$\exp\left(\frac{\omega_b}{T_1}\right) \sim \left(\frac{1 - \cos \beta_0}{1 + \cos \beta_0}\right)^2 \sim 1. \quad (29)$$

Therefore we get  $T_1 \sim \omega_b \ll T_0 \sim \Omega$ , which means, as far as only spontaneous emission of the qubit is concerned, the fluctuation caused by the qubit can be effectively neglected. More realistic estimation of this fluctuation requires detailed information of the quantum noise for the qubit.

The cooling of MR could be measured through the conventional method of motion transduction<sup>35</sup>. In this system, it can also be revealed by the decrease of the integration of the power spectrum for the MR  $\langle z^2(\omega) \rangle$ . Since

$$\delta I = \frac{2\sqrt{2}A\delta\omega}{A^2 + 2\delta\omega^2} \frac{B_0 I_p L_0}{\Delta} \delta z, \quad (30)$$

the power spectrum of the motion is proportional to the power spectrum of the current. The power spectrum of the MR can be read out by the detection of the current in the loop. The current in the flux qubit loop can be recorded through dcSQUID switching measurement or more sophisticated phase sensitive dispersive readout such as Josephson bifurcation measurement<sup>36</sup>.



### Acknowledgement

The authors are very grateful to M. H. Devoret J. E. Mooij, H. Nakano and A. Kemp for their helpful suggestions on the experimental realizations of this proposal. YDW also thank Yong Li, Fei Xue, P. Zhang, F. Marquardt and C. Bruder for fruitful discussions with them. This work is partially supported by the JSPS KAKENHI (No. 18201018 and 16206003).

### APPENDIX: THE DISSIPATIVE DYNAMICS OF THE QUBIT

The dissipative dynamics of the qubit is governed by master equation as

$$\dot{\rho} = -\frac{i}{\hbar} [H_q, \rho] + \mathcal{L}\rho \quad (31)$$

where  $\rho$  is the reduced density matrix of qubit,  $H_q$  is the qubit Hamiltonian in eq. (9) and  $\mathcal{L}$  is the Liouvillian characterizing the influence of environment.

As far as the qubit is concerned, we consider only the spontaneous emission with rate  $\Gamma_0$  because its energy spacing is larger than environment temperature

$$\mathcal{L}\rho = \frac{\Gamma_0}{2} (2\sigma_- \rho \sigma_+ - \rho \sigma_+ \sigma_- - \sigma_+ \sigma_- \rho). \quad (32)$$

By successively applying three unitary transformations to eq. (31)<sup>37</sup> or making use of Fermi golden rule<sup>29</sup>, one can readily obtain the master equation in interaction picture of the rotating frame

$$\dot{\rho}_I^R = \mathcal{L}^R \rho_I^R, \quad (33)$$

where

$$\begin{aligned} \mathcal{L}^R \rho_I^R = & \frac{\Gamma_\downarrow}{2} (2\tilde{\sigma}_- \rho_I^R \tilde{\sigma}_+ - \rho_I^R \tilde{\sigma}_+ \tilde{\sigma}_- - \tilde{\sigma}_+ \tilde{\sigma}_- \rho_I^R) \\ & + \frac{\Gamma_\uparrow}{2} (2\tilde{\sigma}_+ \rho_I^R \tilde{\sigma}_- - \rho_I^R \tilde{\sigma}_- \tilde{\sigma}_+ - \tilde{\sigma}_- \tilde{\sigma}_+ \rho_I^R) \\ & + \frac{\Gamma_\varphi}{2} (\tilde{\sigma}_z \rho_I^R \tilde{\sigma}_z - \rho_I^R), \end{aligned} \quad (34)$$

with

$$\begin{aligned} \Gamma_\downarrow &= \frac{\Gamma_0}{4} (1 + \cos \beta)^2, \\ \Gamma_\uparrow &= \frac{\Gamma_0}{4} (1 - \cos \beta)^2, \\ \Gamma_\varphi &= \frac{\Gamma_0}{2} \sin^2 \beta \end{aligned} \quad (35)$$

and  $\Gamma_0$  is the spontaneous emission rate. This master equation shows that the effective bath formed by the driven qubit in dissipative environment is

$$\exp\left(\frac{\omega_b}{T_1}\right) \equiv \frac{\Gamma_\downarrow}{\Gamma_\uparrow} = \left(\frac{1 + \cos \beta_0}{1 - \cos \beta_0}\right)^2 \quad (36)$$

Therefore, in the interaction picture the equations of motion for the average value of the qubit operators are

$$\begin{aligned} \frac{d}{dt} \langle \tilde{\sigma}_+ (t) \rangle &= -\frac{(\Gamma_\uparrow + \Gamma_\downarrow + 2\Gamma_\varphi)}{2} \langle \tilde{\sigma}_+ (t) \rangle, \\ \frac{d}{dt} \langle \tilde{\sigma}_- (t) \rangle &= -\frac{(\Gamma_\uparrow + \Gamma_\downarrow + 2\Gamma_\varphi)}{2} \langle \tilde{\sigma}_- (t) \rangle, \\ \frac{d}{dt} \langle \tilde{\sigma}_z (t) \rangle &= -(\Gamma_\uparrow + \Gamma_\downarrow) \langle \tilde{\sigma}_z (t) \rangle - (\Gamma_\uparrow - \Gamma_\downarrow). \end{aligned} \quad (37)$$

Setting  $d\langle\sigma_i\rangle/dt = 0$ , we can get the steady-state solution of the qubit in a dissipative system

$$\begin{aligned}\langle\tilde{\sigma}_+\rangle_s &= \langle\tilde{\sigma}_-\rangle_s = 0, \\ \langle\tilde{\sigma}_z\rangle_s &= -\frac{\Gamma_\uparrow - \Gamma_\downarrow}{\Gamma_\uparrow + \Gamma_\downarrow} = -\frac{2\cos\beta(z)}{1 + \cos^2\beta(z)}.\end{aligned}\quad (38)$$

Making use of eq. (38) and the transformation relations eqs. (11), (15) and (17), it turns out that the quantity of our interest in the experimental-frame is related to those in the rotating-frame as

$$\langle\sigma_z\rangle_s = (\cos\theta(z)\cos\beta(z) - \sin\theta(z)\sin\beta(z)\cos\omega_d t)\langle\tilde{\sigma}_z\rangle_s. \quad (39)$$

Neglecting the high-frequency oscillating term, one get the effective value in eq. (20)

$$\langle\sigma_z\rangle_s = -\frac{2\cos^2\beta(z)}{1 + \cos^2\beta(z)}\cos\theta(z) \quad (40)$$

- 
- <sup>1</sup> P. F. Cohadon, A. Heidmann, and M. Pinard, Phys. Rev. Lett. **83**, 3174 (1999).
  - <sup>2</sup> D. Kleckner and D. Bouwmeester, Nature (London) **444**, 75 (2006).
  - <sup>3</sup> M. Poggio, C. L. Degen, H. J. Mamin, and D. Rugar, Phys. Rev. Lett. **99**, 017201 (2007).
  - <sup>4</sup> C. H. Metzger and K. Karrai, Nature (London) **432**, 1002 (2004).
  - <sup>5</sup> S. Gigan, H. R. Bohm, M. Paternostro, F. Blaser, G. Langer, J. B. Hertzberg, K. C. Schwab, D. Bauerle, M. Aspelmeyer, and A. Zeilinger, Nature (London) **444**, 67 (2006).
  - <sup>6</sup> O. Arcizet, R. F. Cohadon, T. Briant, M. Pinard, and A. Heidmann, Nature (London) **444**, 71 (2006).
  - <sup>7</sup> A. Schliesser, P. DelHaye, N. Nooshi, K. J. Vahala, and T. J. Kippenberg, Phys. Rev. Lett. **97**, 243905 (2006).
  - <sup>8</sup> A. Naik, O. Buu, M. D. LaHaye, A. D. Armour, A. A. Clerk, M. P. Blencowe, and K. C. Schwab, Nature (London) **443**, 193 (2006).
  - <sup>9</sup> A. Hopkin, K. Jacobs, S. Habib, and K. Schwab, Phys. Rev. B **68**, 235328 (2003).
  - <sup>10</sup> I. Wilson-Rae, P. Zoller, and A. Imamoglu, Phys. Rev. Lett. **92**, 075507 (2004).
  - <sup>11</sup> I. Martin, A. Shnirman, L. Tian, and P. Zoller, Phys. Rev. B **69**, 125339 (2004).
  - <sup>12</sup> P. Zhang, Y. D. Wang, and C. P. Sun, Phys. Rev. Lett. **95**, 097204 (2005).
  - <sup>13</sup> K. R. Brown, J. Britton, R. J. Epstein, J. Chiaverini, D. Leibfried, and D. J. Wineland, Phys. Rev. Lett. **99**, 137205 (2007).
  - <sup>14</sup> J. E. Mooij, T. P. Orlando, L. Levitov, L. Tian, C. H. v. d. Wal, and S. Lloyd, Science **285**, 1036 (1999).
  - <sup>15</sup> T. P. Orlando, J. E. Mooij, L. Tian, C. H. van der Wal, L. S. Levitov, S. Lloyd, and J. J. Mazo, Phys. Rev. B **60**, 15398 (1999).
  - <sup>16</sup> F. K. Wilhelm and K. Semba, in *Physical Realization of Quantum Computing* (World Scientific, Singapore, 2006).
  - <sup>17</sup> F. Xue, Y. D. Wang, C. P. Sun, H. Okamoto, H. Yamaguchi, and K. Semba, New J. Phys. **9**, 35 (2007).
  - <sup>18</sup> A. Gaidarzhy, G. Zolfagharkhani, R. L. Badzey, and P. Mohanty, Phys. Rev. Lett. **94**, 030402 (2005).
  - <sup>19</sup> A. A. Clerk and S. Bennett, New J. Phys. **7**, 238 (2005).
  - <sup>20</sup> M. P. Blencowe, J. Imbers, and A. D. Armour, New J. Phys. **7**, 236 (2005).
  - <sup>21</sup> P. Poncharal, Z. L. Wang, D. Ugarte, and W. A. d. Heer, Science **283**, 1513 (1999).
  - <sup>22</sup> I. Chiorescu, Y. Nakamura, C. J. P. M. Harmans, and J. E. Mooij, Science **299**, 1869 (2003).
  - <sup>23</sup> S. Saito, M. Thorwart, H. Tanaka, M. Ueda, H. Nakano, K. Semba, and H. Takayanagi, Phys. Rev. Lett. **93**, 037001 (2004).
  - <sup>24</sup> S. O. Valenzuela, W. D. Oliver, D. M. Berns, K. K. Berggren, L. S. Levitov, and T. P. Orlando, Science **314**, 1589 (2006).
  - <sup>25</sup> V. B. Braginsky and S. P. Vyatchanin, Phys. Lett. A **293**, 228 (2002).
  - <sup>26</sup> F. Yoshihara, K. Harrabi, A. O. Niskanen, Y. Nakamura, and J. S. Tsai, Phys. Rev. Lett. **97**, 167001 (2006).
  - <sup>27</sup> K. Kakuyanagi, T. Meno, S. Saito, H. Nakano, K. Semba, H. Takayanagi, F. Deppe, and A. Shnirman, Phys. Rev. Lett. **98**, 047004 (2007).
  - <sup>28</sup> E. Il'ichev and e. al., Phys. Rev. Lett. **91**, 097906 (2003).
  - <sup>29</sup> J. Hauss, A. Fedorov, C. Hutter, A. Shnirman, and G. Schoen, cond-mat/00701041 (2007).
  - <sup>30</sup> K. Karrai, Nature (London) **444**, 41 (2006).
  - <sup>31</sup> M. L. Roukes, in *2000 solid-state sensor and actuator workshop* (2000).
  - <sup>32</sup> A. J. Ferguson, S. E. Andresen, R. Brenner, and R. G. Clark, Phys. Rev. Lett. **97**, 086602 (2006).
  - <sup>33</sup> E. K. Irish and K. Schwab, Phys. Rev. B **68** (2003).
  - <sup>34</sup> F. Marquardt, J. P. Chen, A. A. Clerk, and S. M. Girvin, Phys. Rev. Lett. **99**, 093902 (2007).
  - <sup>35</sup> K. C. Schwab and M. L. Roukes, Physics Today **58**, 36 (2005).
  - <sup>36</sup> I. Siddiqi, R. Vijay, F. Pierre, C. M. Wilson, M. Metcalfe, C. Rigetti, L. Frunzio, and M. H. Devoret, Phys. Rev. Lett. **93**, 207002 (2004).
  - <sup>37</sup> L. Yong, private communication (2007).